NIST Technical Note 1522

Phase Dependence in Radar Cross Section Measurements

Lorant Muth

Institute of Standards and Technology
Administration, U.S. Department of Commerce

NIST Technical Note 1522

Phase Dependence in Radar Cross Section Measurements

Lorant A. Muth
Radio-Frequency Technology Division
Electronics and Electromagnetic Technology Division

September 2001

U.S. Department of Commerce
Donald L. Evans, Secretary

National Institute of Standards and Technology
Karen H. Brown, Acting Director

Certain commercial entities, equipment, or materials may be identified in this document in order to describe an experimental procedure or concept adequately. Such identification is not intended to imply recommendation or endorsement by the National Institute of Standards and Technology, nor is it intended to imply that the entities, materials, or equipment are necessarily the best available for the purpose.

National Institute of Standards and Technology Technical Note 1522
Natl. Inst. Stand. Technol. Tech. Note 1422, 16 pages (September 2001)
CODEN: NTNOEF

U.S. GOVERNMENT PRINTING OFFICE
WASHINGTON: 2000

For sale by the Superintendent of Documents, U.S. Government Printing Office
Internet: bookstore.gpo.gov Phone: (202) 512-1800 Fax: (202) 512-2250
Mail: Stop SSOP, Washington, DC 20402-0001

PHASE DEPENDENCE IN RADAR CROSS SECTION MEASUREMENTS

Lorant A. Muth

Radio-Frequency Technology Division

National Institute of Standards and Technology

Boulder, Colorado 80305

A new measurement and analysis technique to isolate the background signals present in radar cross section measurements is presented. By definition the measured RCS of a target is independent of the measured phase, but it is not independent of the phase difference between the theoretically correct signal and the background error signals present in the measurements. By varying the phase of the theoretical signal and holding the phase of the error signal constant, one can separate these two components.

In the calibration model, where the radar cross section of the calibration target is known, the error signals can be removed from the measurements to obtain an accurate system calibration. When the radar cross section of the target is unknown, only error signals with a constant phase can be removed from the measurements. Error signals that vary in-phase with the theoretical signal will introduce a bias that increases the uncertainty of the measurements.

Key words: measured error fields; measured scattered fields; measured RCS amplitude and phase; radar cross section; RCS

1. Introduction

By definition the radar cross section (RCS) of a target is the squared amplitude of the electric field scattered by a target located at infinity and illuminated by a plane wave. In practice, the reflected electric field is measured monostatically or at a given bistatic angle. In either case, the distance d between a target and the transmitting and receiving antennae is very large, $kd >> 2\pi$, where k is the transmitted wavenumber. The *measured signal* S is composed of a theoretically correct scattered electric field, additional scattered fields that originate from the environment of the measurement range, and distortions due to instrumentation nonlinearity and noise. The measured complex electric field signal S is given by

$$S(r, \theta, b, \beta) = re^{i\theta} + be^{i\beta}, \tag{1a}$$

where r and θ are the amplitude and phase of the reflected electric field signal from the target (that could possibly include in-phase error signals), and b and β are the amplitude

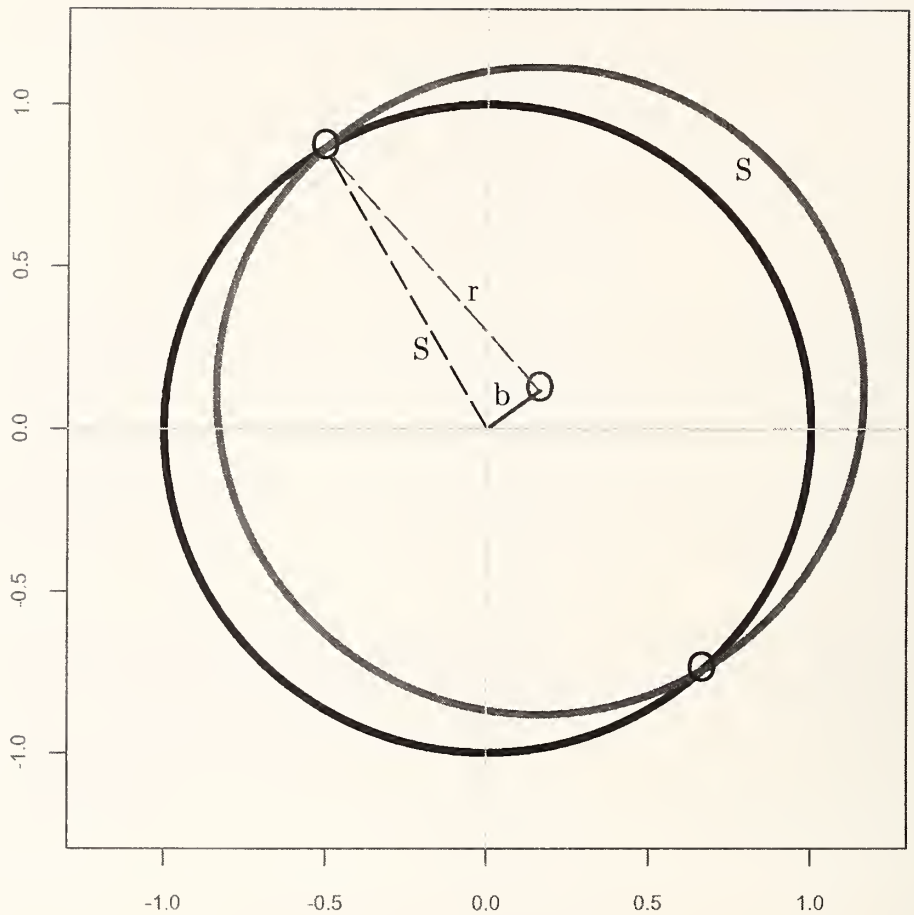

Figure 1. The normalized complex electric field r in *ideal* RCS measurements describes a circle centered on the origin as the phase varies. The background signal $be^{i\beta}$ found in *real* measurements S displaces the center of the ideal circle away from the origin. By removing the background signal from the measurements, RCS calibration accuracy is improved.

and phase of the electric field signal reflected from the environment (which includes calibration and instrumentation effects and noise). The first term in eq (1a) describes a circle in the complex plane centered on the origin as θ varies from 0 to 2π, and the second term is a constant that moves the center of the theoretical circle into the complex plane. Figure 1 illustrates the difference between *ideal* and *real* RCS measurements as modeled in eq (1a). Note that there are two values of the phase $\theta - \beta$ where the measured RCS yields the theoretical value, that is, $S = r$ at these points. These values can be determined easily from the ratio b/r (see below). We can use eq (1a) to formulate simple *measurement- (or data-) based definitions* of r^2, the theoretical RCS, and b^2, the measured background RCS.

Thus,

$$\int_0^{2\pi} S d\theta = 2\pi b e^{i\beta} \tag{1b}$$

and

$$\int_0^{2\pi} |S|^2 d\theta = 2\pi(r^2 + b^2). \tag{1c}$$

Somewhat more complicated expressions result if the integrals in eqs (1b) and (1c) are evaluated between finite angles θ_1 to θ_2 (see Appendix A). These integral equations indicate that we can resolve the signal into a *theoretical RCS* r and *background* b component if we obtain the measurements S as a function of θ. A difficulty here is that the *measured phase* of S, denoted by γ, where

$$\tan\gamma = \frac{r\sin\theta + b\sin\beta}{r\cos\theta + b\cos\beta}, \tag{2}$$

is a nonlinear function of the *unknown* amplitudes r and b and the *unknown* phases θ and β. Moreover, none of the nonlinear parameters of interest in eq (1a) and (2) can be determined independently of S.

A slightly modified formulation can be used to obtain the background signals present in the data. Let $be^{i\beta} = (b_I, b_Q)$; then eq (1a) can be rewritten as

$$(S_I - b_I)^2 + (S_Q - b_Q)^2 = r^2, \tag{3a}$$

where (following accepted usage in the RCS community) the subscripts I and Q denote the real and imaginary components of a complex quantity. The phase θ of r is given by

$$\tan\theta = \frac{S_Q - b_Q}{S_I - b_I}. \tag{3b}$$

Equation (3a) is independent of θ, and is well suited to obtain r^2, the RCS of a calibration or an unknown target, in the presence of a complex background signal b. In Figure 1, the real and imaginary components S_I and S_Q of the electric field data are constrained on a *data circle* with radius r centered at (b_I, b_Q). The *measured* complex electric field S is expressed with respect to the origin, and the fractional measurement error is given by S/r. Obviously, if we can determine and remove the background signal b from the data, the measurement error can be significantly reduced. Experimental realization of this approach is, however, challenging: we need to vary θ without significantly varying β. Variations in β such that $\delta\beta << \delta\theta$ will be incorporated into the overall uncertainty of the measurement. In Section 4 we apply eq (3) to measurements made on a calibration cylinder and sphere and obtain the background signals present in the data.

Finally, we note that only the resultant of many component error signals appears in eq (1). Most of the important sources of error signals found on RCS measurement ranges have been discussed in reference [1], where a general framework of radar cross section uncertainty analysis is presented. A RCS measurement error equation was developed in reference [2]. However, these studies have not demonstrated the magnitude of each of the

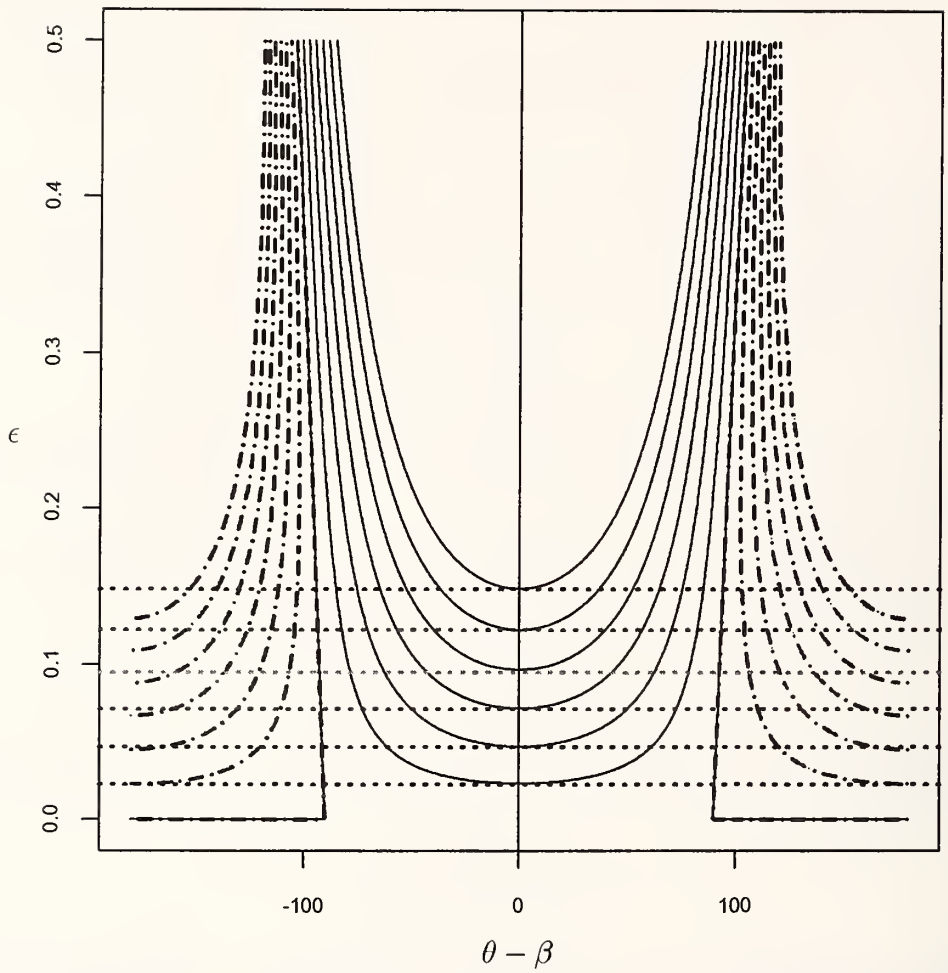

Figure 2. Contours of the RCS measurement error κ^2 as function of the phase $\theta - \beta$ and the dimensionless error parameter ϵ. See eqs (1a), (5) and (6a). Contour lines from -1.2 dB (broken) to $+1.2$ dB (solid) in steps of 0.2 dB are shown. For a given κ the phase $\theta - \beta$ must be specified to uniquely determine ϵ.

specific errors present in real RCS data. To characterize the individual errors (and uncertainties) listed in reference [1], we need to implement experimental procedures specifically designed for the purpose. Measurement programs to accomplish this are in various stages of completion at a number of RCS facilities around the country. In this study, we will not try to determine the component uncertainties of a measurement system, but will concentrate on a *new measurement technique* designed to determine the background signals present in RCS measurements. When such signals are removed from the data the accuracy of RCS calibrations can be significantly improved.

2. Errors in Radar Cross Section Measurements

If in eqs (1) S denotes the calibrated electric field data, then the measured RCS of the target is

$$|S|^2 = r^2\kappa^2(\epsilon, \theta, \beta), \tag{4}$$

where the *error parameter* ϵ is defined as

$$\epsilon \equiv \frac{b}{r}, \tag{5}$$

and the calibration factor κ, (or equivalently, the measurement error) is given by

$$\kappa^2 = 1 + 2\epsilon\cos(\theta - \beta) + \epsilon^2. \tag{6a}$$

We note that if

$$\cos(\theta - \beta) = -\frac{\epsilon}{2}, \tag{6b}$$

then $\kappa = 1$ and $|S| = r$; that is, there is no measurement error. These points are indicated in Figure 1, where the theoretical and shifted circles intersect.

$|S|^2$ is independent of the measured phase γ, but is dependent on the phase difference $\theta - \beta$. Hence, a non-ideal RCS measurement (a measurement that is contaminated by interactions and contributions from the environment and the instrumentation) is *phase dependent*, as seen in eqs (4) and (6a). Finally, in practice one typically expects $\epsilon << 1$, but this is not required in the analysis.

A contour plot of the RCS measurement error κ^2 is presented in Figure 2. Both negative (broken) and positive (solid) contour lines are shown. The contour lines for 0 dB are defined by eq (6b). As the phase difference $\theta - \beta$ varies over all angles, ϵ is seen to vary significantly for a given value of κ. Thus, in addition to specifying κ, we need to specify the phase $\theta - \beta$ to uniquely determine ϵ. In current measurement practice, this phase information is unavailable.

If in eq (1a) S is *uncalibrated* data, then only the ratio of two uncalibrated data sets can be exhibited in a manner similar to eq (4). Thus,

$$\left|\frac{S_2}{S_1}\right|^2 = \left(\frac{r_2}{r_1}\right)^2\left(\frac{\kappa_2}{\kappa_1}\right)^2, \tag{7}$$

where the subscripts denote two independent uncalibrated measurements, and the ratio of measurements removes the system's transfer function from the uncalibrated data set. This equation has the same form as eq (4), if we define

$$S_{21}^2 \equiv \left|\frac{S_2}{S_1}\right|^2, \tag{8}$$

and similarly for the ratios of r_i and κ_i, $i = 1, 2$. Thus,

$$|S_{21}|^2 = r_{21}^2 \kappa_{21}^2 (\epsilon_2, \theta_2, \beta_2, \epsilon_1, \theta_1, \beta_1). \tag{9}$$

Here subscript 1 refers to a calibration artifact, and subscript 2 refers to a target. Explicitly,

$$\kappa_{21}^2 = \frac{1 + 2\epsilon_2 \cos(\theta_2 - \beta_2) + \epsilon_2^2}{1 + 2\epsilon_1 \cos(\theta_1 - \beta_1) + \epsilon_1^2}. \tag{10}$$

Equation (9) has six measurement parameters. κ_{21} is simply the ratio of two uncalibrated measurements S_{21}^2 to the ratio of the corresponding theoretical cross sections r_{21}^2. This ratio gives the *calibrated RCS measurement error* due to all sources of error identified in reference [1]. When r_{21} is known, κ_{21} can be evaluated from the data.

3. The Dual Calibration Technique

The comparison of the ratio of two uncalibrated measurements on two different targets (see eq (8)) to the ratio of the corresponding theoretical RCS values (see eq (9)) yields the *"dual calibration error"* κ_{21} [3]. The theoretical RCSs of the two target artifacts are usually assumed to be known accurately, so that computational errors are negligible in this comparison.

In practice, κ_{21}^2 is usually evaluated using two different-sized simple calibration artifacts such as cylinders or spheres. Typically, dual calibration errors are ± 0.2 dB in the range from 2 to 18 GHz, when comparing two closely-sized cylinders from the standard cylinder set [3,4]. Large errors, on the order of ± 0.4 to ± 0.8 dB, have been observed, especially when cylinders and spheres were compared.

When small values (e.g., up to ± 0.2 dB) of κ_{21} are obtained, the usual interpretation is that a good calibration of the RCS measurement system has been achieved. This conclusion, however, may not be warranted, since, specifying measurement errors without phase information will not uniquely determine the calibration error parameter ϵ_1.

To graphically illustrate κ_{21} with its six measurement parameters, we need to make some simplifying assumptions. First, we make the nonrestrictive and realistic assumption that the phase differences in the calibration and target measurements are the same. Then we assume that $\epsilon_2 = \alpha\epsilon_1$, where α is some arbitrary real constant (which can be varied to explore the behaviour of κ_{21}). For purposes of illustration, we will examine two cases: (i) $\alpha = 1.01$, and (ii) $\alpha = 0.5$. Case (i) represents a simplified model of *repeatability*, and case (ii) is a typical *dual calibration* result. The contours of κ_{21} for these two cases are shown in Figures 3 and 4. Qualitatively, the contour plots for the two cases are similar: for any contour level, ϵ_1 varies significantly as the phase varies. Hence, an independent assessment of the measured phase is needed to determine the error parameters ϵ_1 and ϵ_2 uniquely from a dual calibration result. We observe then that *small dual calibration errors do not necessarily imply small error parameters.*

The *dual calibration error* κ_{21} in eq (9) is simply a *known measurement error* valid specifically for *the two targets under consideration.* Generally valid calibration errors cannot be

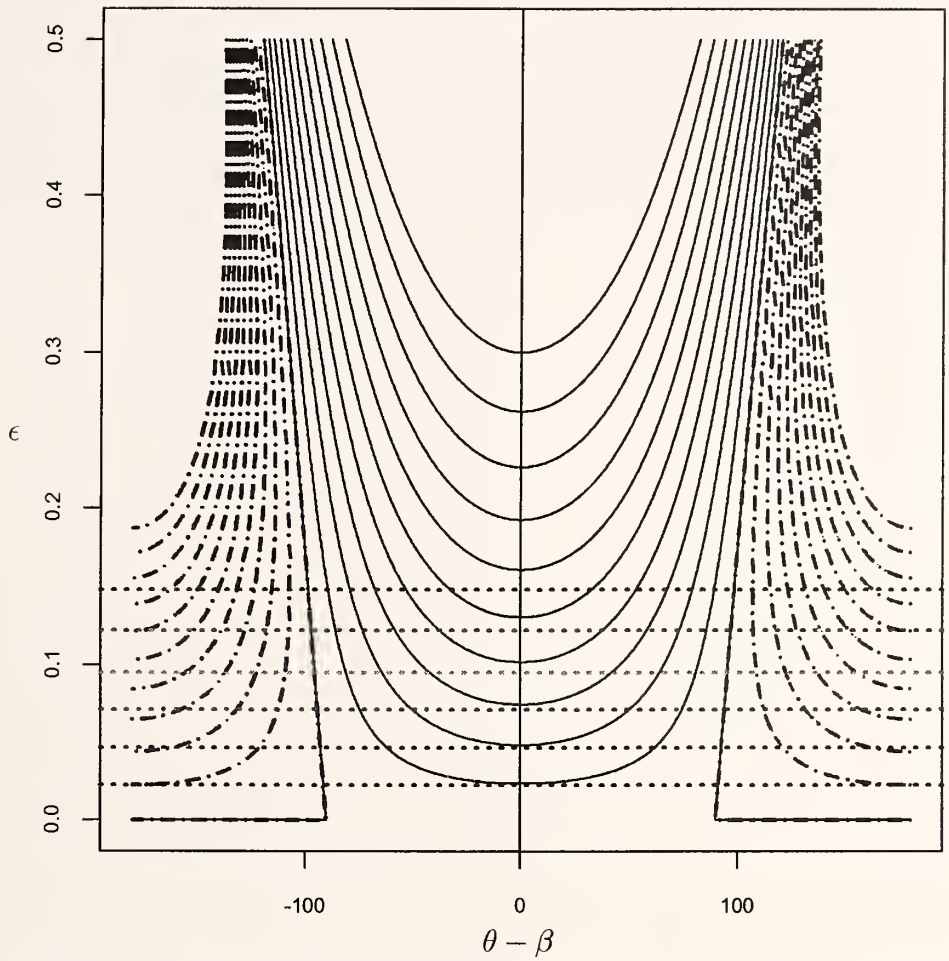

Figure 3. The repeatability of RCS calibrations. Contours of the RCS measurement error κ_{21} as a function of the phase $\theta - \beta$ (assumed the same for both measurements) and the dimensionless error parameters ϵ_1 and $\epsilon_2 = 1.01\epsilon_1$. Contour lines from -0.02 dB (broken) to $+0.02$ dB (solid) in steps of 0.002 dB are shown. For a given κ_{21} the phase $\theta - \beta$ must be specified to uniquely determine ϵ_1.

deduced from such a comparison! The dual calibration technique simply does not provide enough information to determine the error parameters $\epsilon_{1,2}$. We want to determine the *calibration error* ϵ_1, since this error is propagated into all subsequent measurements on real targets.

The dual calibration technique does not determine the calibration error parameters $\epsilon_{1,2}$ uniquely, because important phase information is not available and is not included in the analysis. As indicated in eq (1a), we must specify phase information to determine and remove unwanted errors signals from the data.

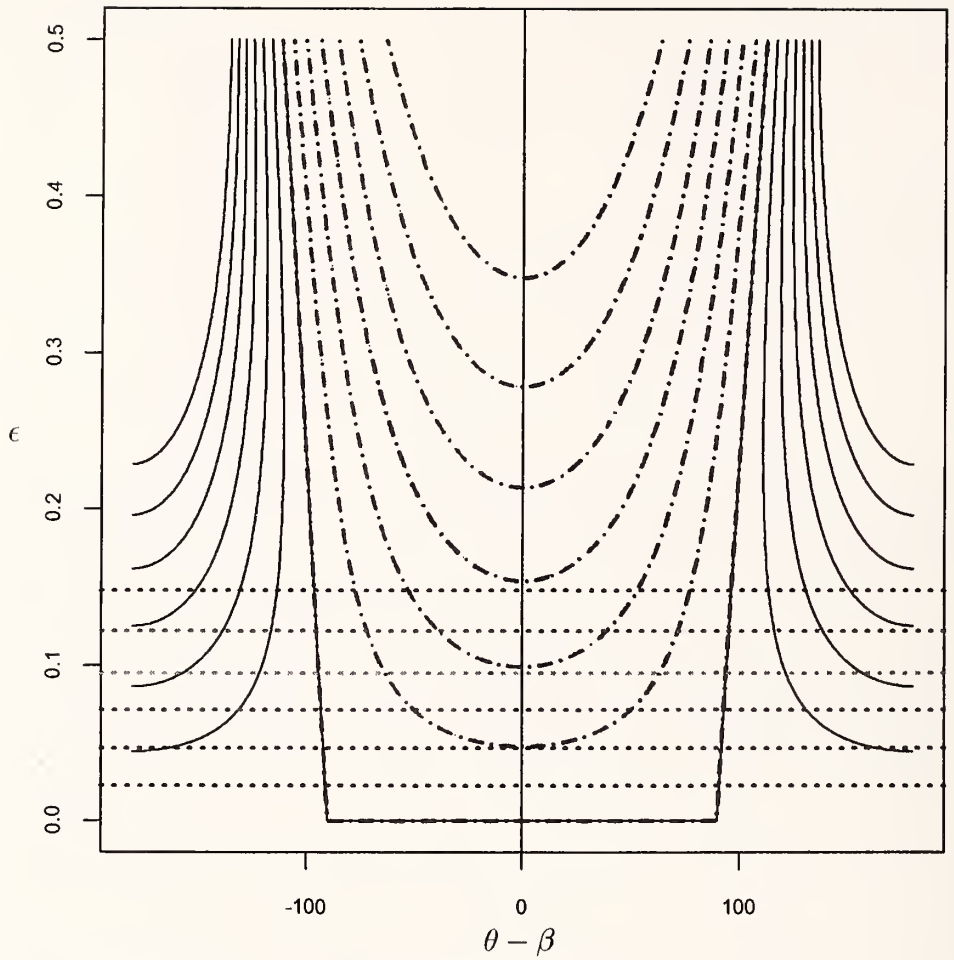

Figure 4. RCS measurement errors. Contours of κ_{21} as a function of the phase $\theta - \beta$ (assumed the same for both measurements) and the error parameters ϵ_1 and $\epsilon_2 = 0.5\epsilon_1$. Contour lines from -1.2 dB (broken) to $+1.2$ dB (solid) in steps of 0.2 dB are shown. For a given κ_{21} the phase $\theta - \beta$ must be specified to uniquely determine ϵ_1.

4. Phase-Dependent RCS Data Analysis

In current practice, a large number of RCS measurements on a *stationary* target are integrated to minimize noise and to reduce the I-Q circularity error in the data. In these measurements, the phase θ in eq (1) is constant for a stationary target, and the two parameters r and b of the received electric field signal S, modeled in eq (1a), cannot be separated. However, the phase

$$\theta = \frac{4\pi}{\lambda} d, \tag{11}$$

where λ is the electromagnetic wavelength, and d is the distance of the target from the radar, will vary from 0 to 2π if we vary the distance d over $\lambda/2$. The resulting variation in the amplitude of the electric field can be safely neglected, since $d/\lambda >> 1$. Given such *phase-dependent data* we can isolate the two parameters of the signal using the method of weighted orthogonal-distance regression [5 – 7].

The orthogonal-distance regression-analysis technique is especially well suited to problems in which all the model variables have significant errors. In eq (10) the quantities (S_I, S_Q) have measurement errors, and we seek to minimize the sum of squares of the orthogonal

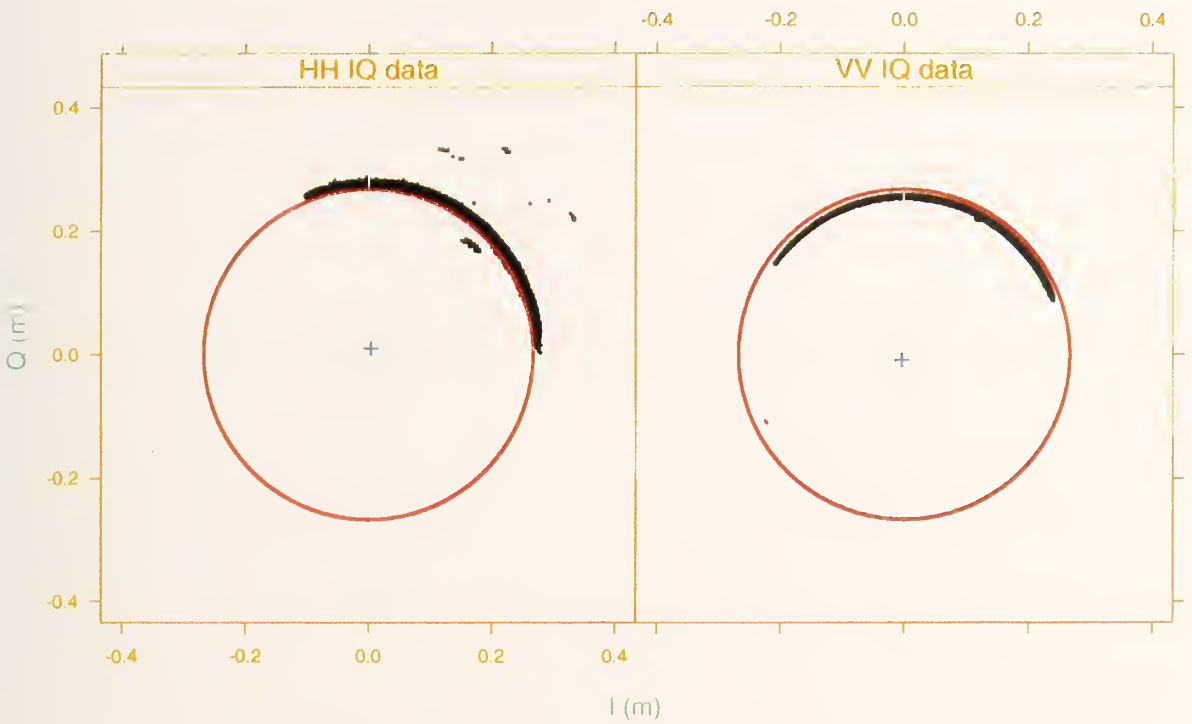

Figure 5. RCS measurements on a 12-inch diameter sphere. The theoretical circles with centers at the origin are mostly above or below the data points. The centers of the data circles (indicated by + signs) have been shifted away from the origins by the background signals. See Figures 1 and 6.

distances between each data point and the circle described by the model equation (10). The correlation between the variables S_I and S_Q are automatically taken into account by the model equation, and the analysis can be used to determine the location of the center of the circle (b_I, b_Q) and the radius of the circle r.

We consider two cases:

i. the *calibration model*, where the RCS of the calibration target r^2 is known,
ii. the *unknown-target model*, where the RCS of the target is unknown.

In this approach, reproducibility of the results, when both models are applied to the same calibration artifact (with known RCS), is easily checked.

Figure 5 shows (S_I, S_Q) data obtained using a 12-inch diameter sphere mounted on a foam column. Both the HH and VV polarizations were measured with a pulse repetition frequency of 5000 s^{-1}. For each polarization approximately 6E+5 data points were recorded; the distance d to the target was ≈610 m. The phase of the data varied approximately 100°, corresponding to a distance variation in the location of the sphere of roughly $\lambda/8 \approx 0.41$ cm at 9.24 GHz. This variation in sphere position was caused by steady and

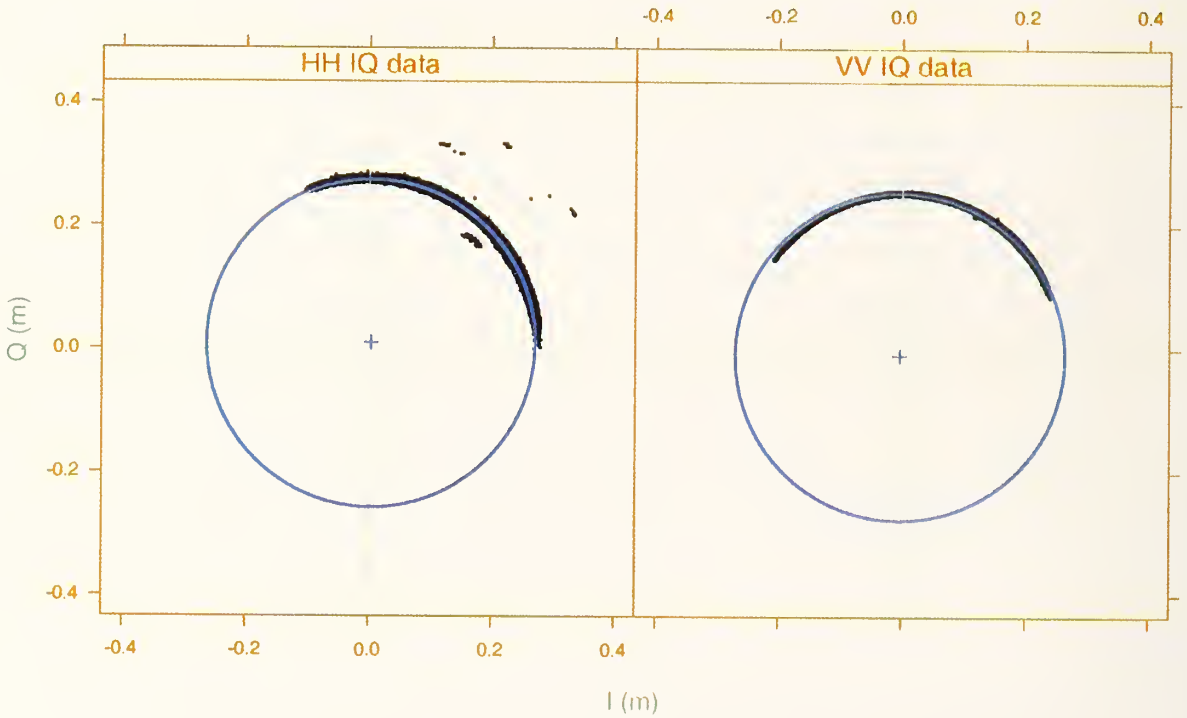

Figure 6. RCS measurements on a 12-inch diameter sphere. The data circles with centers indicated by + signs have been shifted away from the origins by the background signals. The shifted theoretical circles are now embedded in the data. See Figures 1 and 5.

gusting winds of about 20 km/hour. The theoretical RCS of a 12-inch diameter perfectly conducting sphere is $r_0^2 \approx 0.0713$ m^2, or $r_0 \approx 0.267$ m.

In Figure 5 the theoretical circles with radii r_0 are centered at the coordinate origins, and the centers of the data circles, denoted by the + signs, have been translated away from the origins (also see Figure 1). Similar data were obtained for a cylinder 5 in in diameter and 5 in in height; the cylinder data plots are qualitatively similar to the sphere plots, and, therefore, are not shown here.

We used ODRPACK [6] to obtain the centers (b_I, b_Q) and the radius r of the data circles for the calibration cylinder and sphere. We assumed the initial values to be $(0, 0)$ for the centers and the known theoretical values for the radii. In the *calibration model* the theoretical r was held fixed, and in the *unknown target model* both the center and the radius of the circle were allowed to vary to obtain nonlinear least-squares solutions. Uncertainty bounds of 2σ were automatically provided by the code.

Figure 6 shows the (S_I, S_Q) sphere measurements and the centers of theoretical circles shifted away from the origins to minimize the nonlinear-least-squares residuals. Unlike in

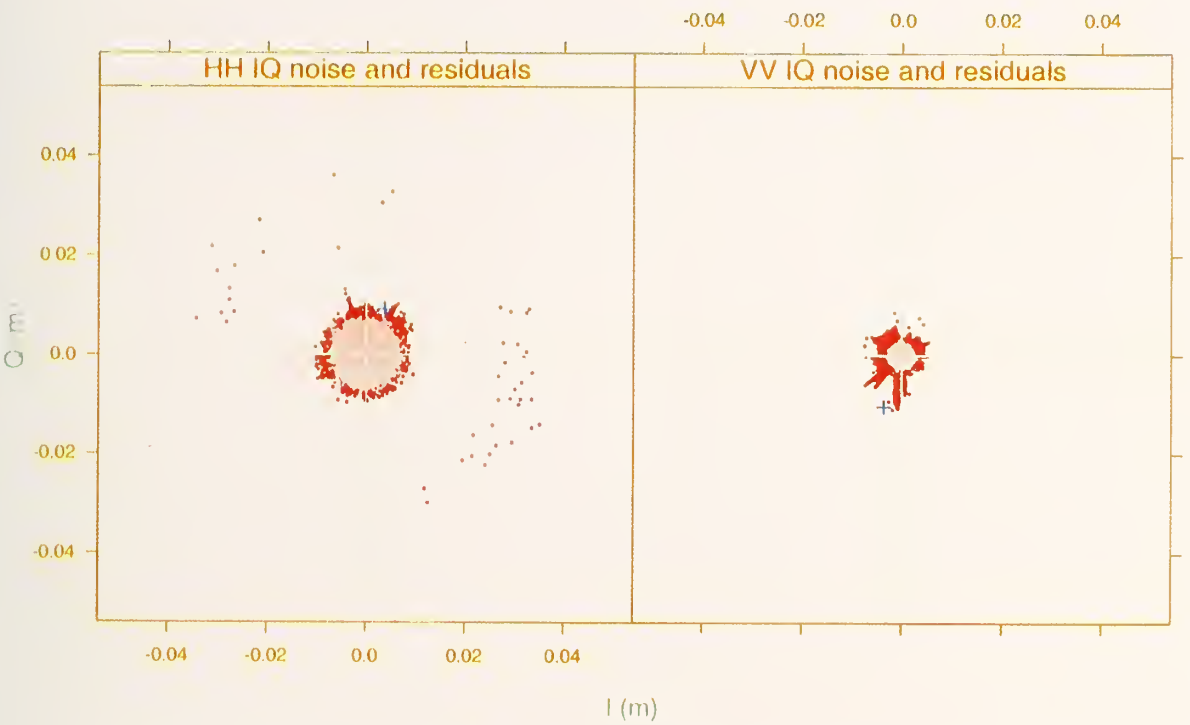

Figure 7. Nonlinear least-squares complex residuals superimposed on the measurement system noise. The residuals are for the solutions shown in Figure 6 with the parameters given in Table 1 for the S_c artifact (calibration model).

Figure 5, the theoretical circle (the calibration model) is now embedded in the data. In Table 1, we show the model parameters with their uncertainties for the sphere and cylinder. Here the subscripts c and t refer to the *calibration* and *unknown target* models, respectively. The uncertainties, indicated in parentheses, are of the order of 1 % or better; that is, all the parameters are well determined. In the *unknown target model*, we find a notable difference between the theoretical values r and the solutions. These systematic (Type B) errors indicate the presence of interactions with the environment and the instrumentation. In Figure 7 we compare the complex system noise with the complex residuals of the nonlinear

TABLE 1. Parameter Solutions* with Uncertainties**
obtained with ODRPACK

Artifact	Channel	I_0	Q_0	r	r_0	ϵ
S_t	HH	$-1.38E-3$	$3.50E-3$	$2.74E-1$	$2.67E-1$	$1.37E-2$
		$(3.90E-5)$	$(4.29E-5)$	$(5.42E-5)$		
	VV	$1.98E-3$	$3.58E-3$	$2.53E-1$	$2.67E-1$	$1.62E-2$
		$(3.14E-6)$	$(6.04E-6)$	$(3.99E-6)$		
S_c	HH	$3.71E-3$	$9.12E-3$	$2.67E-1$	$2.67E-1$	$3.69E-2$
		$(7.83E-6)$	$(7.81E-6)$			
	VV	$-3.64E-3$	$-1.05E-2$	$2.67E-1$	$2.67E-1$	$4.16E-2$
		$(6.10E-6)$	$(4.21E-6)$			
C_t	HH	$2.15E-2$	$9.26E-3$	$4.83E-1$	$4.51E-1$	$4.85E-2$
		$(1.29E-3)$	$(2.90E-4)$	$(1.31E-3)$		
	VV	$1.10E-2$	$1.76E-3$	$4.38E-1$	$4.51E-1$	$2.54E-2$
		$(2.42E-4)$	$(4.16E-5)$	$(2.37E-4)$		
C_c	HH	$-1.06E-2$	$2.50E-3$	$4.51E-1$	$4.51E-1$	$2.41E-2$
		$(1.59E-5)$	$(3.95E-6)$			
	VV	$2.36E-2$	$4.05E-3$	$4.51E-1$	$4.51E-1$	$5.31E-2$
		$(1.24E-5)$	$(6.37E-5)$			

*All quantities in the table are in meters, except for ϵ, which is dimensionless

** $\pm 2\sigma$ uncertainties are shown in parentheses

analysis. The residual amplitudes are seen to be of the same order of magnitude as the noise amplitudes. One can conclude from these plots that the data in Figure 5 are appropriately represented by the nonlinear model equation (10).

5. Future Efforts

In this study we explored a new measurement and analysis technique that allows us to determine the generalized background signal in RCS measurements. This background can be subtracted from the data to improve the accuracy of the calibration or measurement. The results of this study are very encouraging, and warrant further exploration of this measurement and analysis techniques. We need to design and implement experiments where the movement of the sphere (or some other target) is under careful experimental control to demonstrate and support further the validity of the results presented in this study. This should not be difficult, since only very small excursions, of the order of an eighth of a wavelength, are needed. Larger excursions should improve the results, provided we keep β relatively stable. Currently, steps are being taken to repeat these measurements under more controlled conditions.

The author thanks Dr. Dale Diamond and Mr. John Liles at the RCS measurement range at NAWCWD, China Lake, for providing the data used in this study. The author also thanks Mr. John Denson, Deputy Director, NAWCWD and Mr. Dick Dickson, Head, Etcheron Valley Range, NAWCWD for their support and encouragement. The support of the DoD triservice CCG is also acknowledged. The author is appreciative of Dr. Jack C. M. Wang, Statistical Engineering Division, Information Technology Laboratory, NIST, who provided guidance in the use of ODRPACK.

References

[1] Wittmann, R.C; Francis, M.H.; Muth, L.A.; Lewis, R.L. Proposed uncertainty analysis for RCS measurements. Natl. Inst. Stand. Technol. NISTIR 5019, January 1994.

[2] Muth, L. A. Radar cross section calibration errors and uncertainties. Proc., Antenna Meas. Tech. Assoc., Monterey Bay, CA, pp. 115 – 119; 4 – 8 Oct. 1999.

[3] Chizever, H.M.; Soerens, R.J.; Kent, B.M. On reducing primary calibration errors in radar cross section measurements. Proc., Antenna Meas. Tech. Assoc., Seattle, WA, pp. 383 – 388; 30 Sept – 3 Oct. 1996.

[4] Kent, B.M.; Wood, W. D. The squat cylinder and modified bicone primary static RCS range calibration standards. Proc., Antenna Meas. Tech. Assoc., Boston, MA, pp. 319 – 324; 17 – 12 Nov. 1997.

[5] Boggs, P.T.; Rogers, J.E.; Orthogonal Distance Regression. Contemporary Mathematics, 112, 1990.

[6] Boggs, P.T.; Byrd, R.H.; Donaldson, J.R.; Schnabel, R.B. Algorithm 676 – ODRPACK: Software for Weighted Orthogonal Distance Regression. ACM Trans. Math. Software, 15; 1989.

[7] Boggs, P.T.; Byrd, R.H.; Rogers, J.E.; Schnabel, R.B. User's Reference Guide for ODRPACK Version 2.01 Software for Weighted Orthogonal Distance Regression. Natl. Inst. Stand. Technol. NISTIR 4834; June 1992.

Appendix A

The Data Integrals Over a Finite Phase Interval

In eqs (1) we evaluated the data integrals over the range of phase angles:

$$\int_0^{2\pi} S d\theta = 2\pi b e^{i\beta} \tag{1b}$$

$$\int_0^{2\pi} |S|^2 d\theta = 2\pi(r^2 + b^2). \tag{1c}$$

Ordinarily, data are available only over a finite range of θ. The appropriate integrals then become:

$$\int_{\theta_1}^{\theta_2} S d\theta = b e^{i\beta}(\theta_2 - \theta_1) - ir(e^{i\theta_2} - e^{i\theta_1}) \tag{A1}$$

$$\int_{\theta_1}^{\theta_2} |S|^2 d\theta = (r^2 + b^2)(\theta_2 - \theta_1) + 2rb[\sin(\theta_2 - \beta) - \sin(\theta_1 - \beta)]. \tag{A2}$$

These form a simultaneous set of equations that can be solved for the basic parameters r, b, and β, if S is known as a function of θ. We still encounter the difficulty pointed out in the main text. Because only the phase γ of S is known (see eq (2)), these equations are nonlinear in the basic parameters and cannot be solved algebraically.

NIST Technical Publications

Periodical

Journal of Research of the National Institute of Standards and Technology—Reports NIST research and development in those disciplines of the physical and engineering sciences in which the Institute is active. These include physics, chemistry, engineering, mathematics, and computer sciences. Papers cover a broad range of subjects, with major emphasis on measurement methodology and the basic technology underlying standardization. Also included from time to time are survey articles on topics closely related to the Institute's technical and scientific programs. Issued six times a year.

Nonperiodicals

Monographs—Major contributions to the technical literature on various subjects related to the Institute's scientific and technical activities.

Handbooks—Recommended codes of engineering and industrial practice (including safety codes) developed in cooperation with interested industries, professional organizations, and regulatory bodies.

Special Publications—Include proceedings of conferences sponsored by NIST, NIST annual reports, and other special publications appropriate to this grouping such as wall charts, pocket cards, and bibliographies.

Applied Mathematics Series—Mathematical tables, manuals, and studies of special interest to physicists, engineers, chemists, biologists, mathematicians, computer programmers, and others engaged in scientific and technical work.

National Standard Reference Data Series—Provides quantitative data on the physical and chemical properties of materials, compiled from the world's literature and critically evaluated. Developed under a worldwide program coordinated by NIST under the authority of the National Standard Data Act (Public Law 90-396). NOTE: The Journal of Physical and Chemical Reference Data (JPCRD) is published bi-monthly for NIST by the American Chemical Society (ACS) and the American Institute of Physics (AIP). Subscriptions, reprints, and supplements are available from ACS, 1155 Sixteenth St., NW, Washington, DC 20056.

Building Science Series—Disseminates technical information developed at the Institute on building materials, components, systems, and whole structures. The series presents research results, test methods, and performance criteria related to the structural and environmental functions and the durability and safety characteristics of building elements and systems.

Technical Notes—Studies or reports which are complete in themselves but restrictive in their treatment of a subject. Analogous to monographs but not so comprehensive in scope or definitive in treatment of the subject area. Often serve as a vehicle for final reports of work performed at NIST under the sponsorship of other government agencies.

Voluntary Product Standards—Developed under procedures published by the Department of Commerce in Part 10, Title 15, of the Code of Federal Regulations. The standards establish nationally recognized requirements for products, and provide all concerned interests with a basis for common understanding of the characteristics of the products. NIST administers this program in support of the efforts of private-sector standardizing organizations.

Consumer Information Series—Practical information, based on NIST research and experience, covering areas of interest to the consumer. Easily understandable language and illustrations provide useful background knowledge for shopping in today's technological marketplace.
Order the **above** *NIST publications from: Superintendent of Documents, Government Printing Office, Washington, DC 20402.*
Order the **following** *NIST publications—FIPS and NISTIRs—from the National Technical Information Service, Springfield, VA 22161.*

Federal Information Processing Standards Publications (FIPS PUB)—Publications in this series collectively constitute the Federal Information Processing Standards Register. The Register serves as the official source of information in the Federal Government regarding standards issued by NIST pursuant to the Federal Property and Administrative Services Act of 1949 as amended, Public Law 89-306 (79 Stat. 1127), and as implemented by Executive Order 11717 (38 FR 12315, dated May 11, 1973) and Part 6 of Title 15 CFR (Code of Federal Regulations).

NIST Interagency Reports (NISTIR)—A special series of interim or final reports on work performed by NIST for outside sponsors (both government and non-government). In general, initial distribution is handled by the sponsor; public distribution is by the National Technical Information Service, Springfield, VA 22161, in paper copy or microfiche form.

★US GOVERNMENT PRINTING OFFICE: 2001 — 845-691

U.S. Department of Commerce
National Institute of Standards and Technology
325 Broadway
Boulder, Colorado 80305-3337

Official Business
Penalty for Private Use, $300